

## Advanced GPSR in Mobile Ad-hoc Networks (MANETs)

<https://doi.org/10.3991/ijim.v14i18.16661>

Mohammad M. Alnabhan  
Mutah University, Mutah, Jordan  
m.alnabhan@mutah.edu.jo

**Abstract**—This work aims to develop the routing capability of GPSR in MANETs. A new GPSR improvement described as Advanced GPSR (AGPSR) is proposed with enhanced greedy forwarding and efficient routing decision. AGPSR greedy forwarding model consists of three major phases; initialization, finding target neighbor, weight value computation and next hop selection. The weight value encounters a set of network metrics including node density, network size, congestion level, transmission range, node speed and movement direction. An intensive evaluation methodology was implemented in order to evaluate the performance of proposed AGPSR in MANET. Results confirm that proposed GPSR has surpassed several MANET environmental challenges and outperformed conventional GPSR in terms of PDR, E2E delay, routing overhead, and power consumption. The delay is reduced by AGPSR of up-to 10% compared to conventional GPSR. In addition, 5% increase in PDR and more than 7% decrease in routing overhead and in power consumption was achieved by AGPSR.

**Keywords**—GPSR; MANET; QoS; PDR; E2E delay; NRL

### 1 Introduction

MANET is an infrastructure-less wireless network, allowing nodes to be involved in the routing process. MANET routing performance is affected by capabilities of mobile nodes and reliability of routing protocol used [1]. MANETs routing protocols are mainly classified into geographic routing protocols also known as location-based routing protocols, and topology-based routing protocols. Topology-based protocols are classified further as reactive or proactive protocols. Proactive routing is considered reliable due to high route availability and limited latency [2]. However, overhead incurred from routes pre-construction and maintenance will limit routing scalability of proactive protocols, and will consume lot of memory resources as the network size grows. An example of proactive routing protocols is Destination Sequenced Distance Vector protocol (DSDV) [3]. Reactive routing consumes less resources comparing to proactive protocols. However, the on-demand route discovery process may fail or take long time to find the required route in sparse network areas and when nodes mobility is very high. This will increase the latency and packet loss, hence degrade overall routing performance. Ad hoc on Demand Distance Vector routing (AODV) are examples of reactive routing protocols [4]. The last type of topology-based protocols is known as hybrid

protocols which combines properties of reactive and proactive routing protocols. Zone Routing Protocol (ZRP) is an example of hybrid protocols [5].

In the other hand, position-based routing protocols perform its routing decision based on knowledge of geographical position of neighboring nodes. Each node within the network will determine its own location information using a Global Position System (GPS) device or any localization method [6]. Hence, to make effective routing decisions each node needs to maintain accurate position information of at least its direct neighbors. For this reason, a short beacon packet is intermittently broadcasted by each node, to announce its existence and location to its neighbors, within its transmission range. Information contained in beacon packets is recorded by receiving nodes in their lists of neighbors and used for forwarding packets to destination. Basically, each node will forward a packet to one of its neighboring nodes which is nearest to the destination.

This is known as the greedy forwarding mechanism [7, 8]. Generally, position-based routing protocols scales much better than topology-based protocols especially in high density environment and increased network size in MANETs, because it does not require to have up-to-date view of network topology and detailed routing table. However, only current physical location of the nodes is required. This advantage will reduce the extra overhead imposed by topology constraints for route discovery [9, 10].

A wide variety of position-based routing protocols was introduced, this includes: Greedy Perimeter Stateless Routing (GPSR), Greedy Routing protocol (GFP), Location Aided Routing Protocol (LAR), Directional Greedy Routing Protocol (DGRP), and Mobility-based Adaptive Greedy Forwarding (MAGF) [11]. GPSR is considered one of most efficient and reliable routing protocols in MANETs. GPSR defines neighboring nodes as nodes within the transmission range and with one hop distance. GPSR utilizes greedy forwarding method to forward packet to next hop node. However, if greedy forwarding was not successful to find a neighbor closer to the destination than itself, this forms a void in a planarized network graph. Hence, GPSR protocol shifts to the perimeter forwarding strategy and uses right-hand rule to overcome this problem [12, 13, 14]. Although of enhanced GPSR routing capabilities, it still suffers from several limitations such as; greedy forwarding failure due to sparse networks and non-uniformly distributed nodes. In the same concern, location inaccuracy, will disconnect the graph causing packet lost, which results in decreased packet delivery ratio [15]. In addition, continuous updates of location information will result in high network overhead and congestion. Hence, using only distance to destination as the only selection criteria of next hop node is not efficient enough for greedy forwarding to scale well in all network conditions and environments.

This research work addresses limitations of GPSR protocol in MANET domain. The aim is to develop GPSR to be more scalable and reliable in all MANET environmental conditions. The proposed model considers node movement speed and direction, network density, node congestion level and transmission range in the routing decision. This allows GPSR to account for dynamic topology changes and mobile node capabilities, in order to achieve optimal routing performance. This work is structured as follows; section 2 describes literature review and related work; section 3 presents details of proposed Advanced GPSR (AGPSR) algorithm. Section 4 describes the evaluation

study conducted and section 5 presents and discusses achieved results. Section 6 concludes this work.

## **2 Literature**

Several studies have investigated the performance of topology-based and position-based routing [16]. In [17], topology-based routing protocols including AODV, DSR and DSDV were analyzed and evaluated. Results confirm that AODV and DSR are more reliable and outperform DSDV. A similar study conducted by [14], which have indicated that DSDV outperforms both DSR and AODV protocols in terms of Packet Delivery Ratio (PDR) and packet loss. However, AODV achieved advanced performance comparing to DSDV and DSR in terms of average throughput. In [2], a set of routing protocols from both MANET protocols categories were investigated, this includes; AODV and DSR from Topology-based protocols, and Geographic Source Routing (GSR) and GPSR for Position-based routing protocols. Results achieved have illustrated different levels of performance; where GSR and GPSR reported lowest PDR using Constant Bit Rate (CBR) rate. However, in terms of latency, GSR performed the best.

In [10], a set of MANET protocols including; DSDV, DSR, ZRP, and position-based greedy protocol (PDGR) were evaluated in terms of PDR, End to End (E2E) delay, and routing overhead. Results achieved have proven that PDGR outperformed topology-based protocols (DSDV, DSR and ZRP) in high dynamic and dense environments. In the same concern, [18] evaluates the efficiency of Location-aided Routing (LAR), Distance Routing Effect Algorithm for Mobility (DREAM), and AODV. LAR and DREAM are position-based routing protocols and the rest are topology based. All these protocols were evaluated using a hierarchical evaluation methodology where a set of simulation scenarios were used representing sparse, dense, dynamic and static environmental conditions. Results have confirmed that LAR protocol outperformed DREAM protocol in terms of all performance metrics except for energy consumption.

In [8], the performance investigation was focused only towards location-based routing protocols, this includes; GPSR, Energy Aware Geographic Routing (EGR), LAR, and DREAM. Performance metrics considered were network lifetime, delay, PDR and energy consumption. EGR and GPSR protocols outperformed other protocols in all performance metrics. EGR performs best in terms of delivery ratio and network lifetime. However, GPSR outperformed EGR in energy consumption and delay. In addition, [19] investigates the performance of GPSR and AOMDV protocols in a Mobile Wireless Sensors Networks (MWSNs) which implements a similar environment to MANET.

Performance metrics used were PDR, routing overhead, hop count, and energy consumption. It was confirmed that GPSR, outperforms AOMDV due to its lower routing protocol overhead. A similar study was conducted in [20], where the performance of GPSR was compared to ZRP in a VANET environment. Results show that GPSR is superior compared to ZRP in terms of PDR, E2E delay, and packet loss. In the same concern, an intensive performance comparison of GPSR and Optimized Link State Routing protocol (OLSR) in Airborne Ad-hoc Networks, was conducted in [21]. The

focus was on analyzing UDP and TCP traffic, where results have shown that GPSR performed the best in terms of E2E delay, and OLSR achieved better results in terms of throughput.

Several evaluation studies have indicated that position-based routing algorithms outperforms topology-based routing in different MANET environments. This is due to a set of operational and functional advantages. Using position-based protocols, nodes are not required to maintain and update routing tables. Where routing process is accomplished based on local information at each sender node. However, greedy forwarding, which is the primary packet forwarding method used by position-based routing, may fail in several conditions such as low density and sparse networks, or networks with voids constructed. This limits the capability of greedy forwarding in guaranteeing packet delivery to the required destination. In addition, performance of position-based routing is degraded from nodes' location inaccuracy. This is due to nodes' mobility, continuous topology changes and infrequent time interval of beacon packets between MANET nodes [22]. Hence, location measurements suffer from error sources which in turn effects the routing decision. Other limitations exist in position-based routing protocols. This includes disconnection due to limited node coverage, incorrect edge removal by planarization, and permanent routing loops due to planarization failure of not removing edge [23, 24].

In order to improve performance of position-based protocols, more especially GPSR, several solutions were presented. In [25] the impact of node mobility and beacon packets interval on position information accuracy was investigated while utilizing GPSR protocol. Afterwards, mobility prediction model was presented to improve its routing decisions accuracy and reliability. An improved GPSR protocol was proposed in [26], in which the focus was on developing a reliable next hop node selection mechanism which considered factors such as distance and movement direction of next-hop candidate nodes. Consequently, [27] presented an extension of GPSR protocol, known as Prediction based Greedy Perimeter Stateless Routing (PGPSR). This protocol extension focused on developing the structure of hello and query packets, it also introduced new mechanism to predict the position of mobile node and new network topology structure. It was confirmed that PGPSR adapt to high speed mobility and continuous topology changes, and allows the selection of optimal next hop. However, limitations of mobility prediction models include high implementation cost, and its un-optimal mobility node motion assumptions.

In addition, [28], improved GPSR by including additional information in neighbors table to assist in selecting next hop more efficiently. This advancement was described as Adaptive GPSR and proved to avoid link breakage and outperformed conventional GPSR in terms of hop count and PDR. Similarly, [29] introduced an extension of GPSR, known as Path-Aware (PA-GPSR), which was implemented in a VANET environment to overcome some of GPSR limitations such as link-breakage. Results reported confirmed that PA-GPSR outperformed conventional GPSR in terms of packet loss, E2E delay, and routing overhead. An additional version of GPSR, known as Density and Velocity Aware GPSR (DVA-GPSR) was presented in [30]. The implementation of this protocol was focused on VANET environment where density and speed of vehicles were utilized to provide a context aware GPSR that outperformed conventional GPSR

in terms of PDR, throughput and routing overhead. A new version of GPSR was presented in [31], in a challenging environment, described as shipborne Ad-hoc network. This GPSR update was based on utilizing variables such as direction, density and proximity of ships. Results reported have shown that new GPSR achieved improved PDR performance.

Accordingly, the performance of GPSR in MANET and VANET environments has been widely investigated in previous research. In addition, GPSR adaptation within these environments was considered in several studies to improve its routing scalability and efficiency, allowing GPSR to respond quickly to high mobility, and dynamic topology changes. However, most previous studies have conducted their evaluation work with single view without considering all environmental settings. In addition, improved versions of GPSR have focused on limited context features, allowing GPSR to achieve improved performance in particular domains only.

This work analyzes the shortcomings of GPSR and propose a new method to develop its greedy routing strategy, by taking into consideration several influencing factors such as nodes' movement speed and direction, nodes' available buffer space and congestion, and nodes' radio range. These factors were used to construct weight values for each neighboring node, in order to assist in selecting optimal next hop nodes. Hence, an Advanced GPSR (AGPSR) routing strategy was introduced in this work considering all MANET constrains. A constructive and hierarchal evaluation methodology implementing all possible MANET settings, was utilized to evaluate the performance and efficiency of proposed AGPSR.

### **3 Proposed AGPSR Greedy Forwarding Strategy**

This work investigates the routing capability and performance of GPSR. The focus is on GPSR greedy routing strategy, in which a new weight-based mechanism was adopted for more efficient routing decision. The weight mechanism is used to select next hop neighbor node based on a set of performance metrics related to network and mobile nodes. These performance metrics are divided into two groups:

- The first group is related to route reliability and efficiency and consists of several variables including; node density, network size, congestion and connectivity, and transmission range. Where route reliability is the availability of stable route to destination with required time period. Route efficiency refers to delivery of data to final destination with minimum delay and lowest loss.
- The second group is related to node mobility and consists of four variables; node speed, movement direction, distance to sink and beacon update interval. This group of variables is used to encounter for node mobility challenges and accurately predicting distance to destination.

These performance metrics are interrelated of each other. For example, high node density will result in increased connectivity, throughput and transmission ranges. This will reduce the number of hops to reach the destination and will decrease the probability of wireless link breakage, hence improve reliability and stability of communication

routes. However, high node density will increase network overhead and congestion level, which result in reduced route efficiency. In addition, increased density will rise power consumption reducing network life time which in turn negatively affects route stability. Node density is also affected by network size, in which large network size will surpasses the positive affect of network density. In addition, node mobility includes movement speed and direction, which dramatically change network topology and affects route stability. Also, if nodes move outside the transmission range of sender this will cause link breakage and loss of connectivity. Accordingly, balance and optimization of these performance metrics are vital tasks to be considered while chosen next hop node in greedy forwarding. These performance metrics are computed periodically at each node and are broadcasted using beacon packets. Each sender node will use beacon information to update its routing table and compute a weight value for each neighbor node. This weight value is used to select most stable and least congested route providing lowest end-to-end delay and highest throughput. The computation of this weight value is described in the following section.

### 3.1 Route reliability and efficiency factors:

- a) **Node density, network size and transmission range:** The term node density, refers to the number of nodes distributed within a certain area. However, the distribution of nodes is not normal around each node. Node density can influence routing behavior and performance in WSN and MANETs. In which, nodes transmit and route data traffic based on its connectivity with neighboring nodes. However, high node density is considered unfavorable for energy consumption and result in congestion and collision, and might degrade overall network efficiency. Generally, node density is computed by measuring number of nodes over a particular area. This can be represented as follows [32]:

$$D = \frac{N}{A} \quad (1)$$

Where  $D$  denotes node density,  $N$  denote number of nodes and  $A$  is the network grid size represented by the  $x$  and  $y$  area dimensions. Large network size reduces positive effect of dense networks, because hop count to destination will increase and node connectivity will be reduced, which will negatively affect route stability. This provides the attention concerning the population around each node known as node neighbors. High number of neighbors enhances node connectivity and allow obtaining redundant and stable routes to the destination. Node connectivity level, denoted as  $C_n$ , can be measured by computing the average number of its surrounding neighbors  $R_n$ . This is presented as follows:

$$C_n = R_n \quad (2)$$

Several factors are related to node density; this include node mobility, network size, and transmission range. The transmission range effects node connectivity with its neighbors. Long transmission range increases overall connectivity and reduces hop

counts. Short transmission range increases probability of link breakage between neighbors. In dense network, too many communication links and high transmission ranges exists. This will reduce the number of hops to destination, hence average route length will be short and within sender's radio range. This increases route stability and links are less likely to break due to node mobility. In order to provide a complete understanding of network context and nodes deployment, a factor known as node degree can be used to accommodate node density and radio rang. Node degree can be presented by the following equation [32]:

$$\mu = D\pi r^2 \quad (3)$$

Where  $\mu$  is node degree,  $D$  is the node density, and  $r$  is the radio transmission range.

b) Node congestion: Congestion at node  $n$  is measured using Buffer Occupancy Ratio [33], which is the ratio between occupied queue size and overall buffer size at a predetermined time.

$$B_n = \frac{\text{Occupied Buffer Size}}{\text{Buffer Length}} \quad (4)$$

After estimating buffer occupancy ratio  $B_n$ , De-congestion level  $G_n$  at node  $n$  is computed as follows [34]:

$$G_n = 1 - B_n \quad (5)$$

Hence, the node is considered fully congested if de-congestion level ( $G_n$ ) is (zero) 0, and mostly available and away from being congested if de-congestion level ( $G_n$ ) is closer to (one) 1.

### 3.2 Node mobility factors:

a) Node speed, movement direction, and distance to sink: Mobility is a fundamental feature of sensor nodes either in MANETs or WSN. Mobility is related to node speed and movement direction. Mobility impacts topology deployment, density levels, and plays a major role in the reliability of routing in MANET. High node mobility results in rapid topology changes, this will progressively increase probability of link failure, which leads to retransmission of packets and increased communication overhead. Hence, power consumption, delay and congestion will be increased. Link failure will be caused due to two reasons; nodes will move outside the transmission range of senders and nodes will die due to battery termination.

As mentioned earlier, the selection of next-hop node in greedy forwarding is based on measuring the distance between neighbor nodes and destination node (sink), in which, closest neighbor is selected. Hence, in greedy forwarding, it is important to consider mobility constraints such as node velocity and movement direction to accurately estimate the location of the sender node, next-hop candidate, and sink, for guaranteeing routing efficiency. Formulas (6) and (7) are used to compute updated x and y coordinates at current time t1 for node  $n$  (were destination d is a fixed sink), taking into consideration node  $n$  fixed velocity  $v_n$  [35]:

$$x_{t1} = \Delta t * v_n * \cos(\varphi) + x_{t0} \quad (6)$$

$$y_{t1} = \Delta t * v_n * \sin(\varphi) + y_{t0} \quad (7)$$

Where  $\cos(\varphi)$  and  $\sin(\varphi)$  are horizontal and vertical movement directions respectively, and  $(x_{t0}, y_{t0})$  are previous location coordinates measured at  $t_0$ . However, if node  $n$  will have different speeds and accelerations, equations (8) and (9) are used to compute updated  $x$  and  $y$  coordinates at current time  $t_1$  [35]:

$$x_{t1} = \Delta t * v_{n,t1} * \cos(\varphi) + x_{t0} + \frac{1}{2} a_{n,x1}^2 \Delta t^2 \quad (8)$$

$$y_{t1} = \Delta t * v_{n,t1} * \sin(\varphi) + y_{t0} + \frac{1}{2} a_{n,y1}^2 \Delta t^2 \quad (9)$$

Where  $a_{n,x1}, a_{n,y1}$  are the acceleration of node  $n$  at current time  $t_1$  in the horizontal and vertical axis respectively, and are computed as follows:

$$a_{n,x1} = a_{n,t1} \cos(\varphi) \quad (10)$$

$$a_{n,y1} = a_{n,t1} \sin(\varphi) \quad (11)$$

For enhance link stability in greedy forwarding, it is important to measure relative velocity between source node and next-hop neighbors. High difference in relative velocity indicates that nodes are traveling a greater distance either in the same or opposite direction from each other. This will increase the possibility of link breakage between source node and next-hop node. Hence, choosing neighbor nodes with less relative velocity increases the reliability of communication link and allows connectivity to last for a longer duration.

Consider both source node  $S$  and candidate neighbor  $n$  are traveling in dissimilar directions. Consequently, an angle  $\theta$  exists between  $S$  and  $n$ . Three movement cases between  $S$  and  $n$  can be attained based on  $\theta$  [36, 26]:

- $\theta$  is between 0 or 180, in which  $S$  and  $n$  are moving in different directions and in different area zones.
- $\theta = 0$ , specifies that  $S$  and  $n$  are moving within a similar area and at the same direction.
- $\theta = 180$ , specifies that  $S$  and  $n$  are moving in a similar area, however in an opposite direction.

The relative velocity is computed based on  $\theta$  and cosine law as shown below [36]:

$$V_{sn} = \begin{cases} v_s - v_n & \theta = 0 \\ v_s + v_n & \theta = 180 \\ \sqrt{v_s^2 - 2v_s v_n \cos\theta + v_n^2} & \theta \neq 180 \end{cases} \quad (12)$$

Where  $V_{sn}$  is relative velocity between  $n$  and  $S$ .  $v_n$  is the velocity of neighbor node  $n$ ,  $v_s$  is the velocity of the source node  $S$ .

b) Beacon Update Interval (BUI): Mobility of nodes will cause location measurement inaccuracy, more especially if beacon messages were not broadcasted periodically enough ensuring availability of updated location information between neighbors. For example, when a sender node selects its next-hop at time  $t_0$ , this later may not be available at time  $t_1$  (time of transmission) because it has moved, or another neighbor node closer to sink was not detected by sender. This may be the reason behind the obsolete location information stored in routing table at neighboring nodes. Hence, to overcome impact of mobility on location accuracy, beacon updates should take place in a time frame with reference to nodes' speed taking into consideration not to overwhelm the network with beacon messages. In this work, Beacon Update Interval (BUI) is computed at source node and is linked to relative velocity as described below:

$$BUI = \frac{\text{Default Update Interval}}{V_{sn}} \quad (13)$$

BUI is an on-demand update interval in which a new beacon packet will be requested by source node from neighbor node on the bases of BUI. If relative velocity is very high BUI will be very short and beacon packet will be requested very often. If relative velocity is very low (i.e. below 1), and BUI value is almost the value of default beacon interval, then no extra beacon packets are requested from neighbor node [35, 24].

### 3.3 Adaptive greedy forwarding algorithm

The proposed adaptive greedy forwarding mechanism is used to ensure the accuracy and validity of routing table and maintain efficient routing performance. The pseudocode of the proposed mechanism is described in figure 1. Three major operational phases were introduced allowing source node  $S$  to select next forwarding node reaching target destination  $d$  using optimal route. The first phase described as initialization phase, in which each source node  $S$  lockup its routing table to find latest beacon packets received from its neighboring nodes. Nodes with one hop distance from  $S$ , also exchanging routing updates with  $S$  and within its radio range are defined as  $S$  neighbors. Content of beacon packet used in proposed model is described in the following section. Step 1 in pseudocode describes the initialization and update phase. Steps 2 to 20 describes the operations conducted at phase I which is responsible for finding target neighbors, which are neighbor nodes achieving distance and direction conditions. Phase II, is responsible for creating a weight matrix for target nodes, selecting next hop node and make the routing decision. Phase III is designated in step 21 through to step 31 as shown in figure 1.

```

Algorithm: Adaptive-Greedy-Forwarding (Packet)
1:  $R_S$ : Set of neighbor nodes' for S.
//Phase 2: Find target neighbors of source S.
2: While ( $n \in R_S$ )
3:  $D_n^d = \text{DISTANCE}(P_n, P_d)$  //Equ.14,15
4:  $D_r = \text{RATIO}(D_n^d, D_S^d)$  //Equ.16
5: If ( $D_r < 1$ )
6:  $N_D \leftarrow n$  //  $N_D$ : Set of nodes closer to destination
than source S.
7: End if
8: End While
9: If ( $N_D == 0$ ) //No nodes closer to destination
found
10: Forward.Mode = Perimeter //Change to Perimeter
mode
11: Return Greedy-Forward-Failure
12: Break
13: End If
14: While ( $n \in N_D$ )
15:  $Dir(n, d) = \text{DIRECTION}(D_n^d)_{t0,t1} * A(n, d)_{t0,t1}$  //Equ.17,18
16:  $Dir_r = \text{RATIO}(Dir(n, d)_{t0}, Dir(n, d)_{t1})$  //Equ.19
17: If ( $Dir_r < 1$ )
18:  $T \leftarrow n$  //T: Set of target nodes for source s.
19: End if
20: End While //Phase 3: Create weight matrix and
select next hop.
21: While ( $n \in T \ \& \ N_D$ )
22:  $Weight(n) = \frac{1}{v_{sn}} + G_n + C_n$ 
23:  $W_{matrix} = \{n.Weight(n)\}$  //  $W_{matrix}$  is weight matrix.
24: End While
25:  $W_{max} = 1$  //  $W_{max}$  is the maximum weight value.
26: While ( $n \in W_{matrix}$ )
27: If  $Weight(n) \geq W_{max}$ 
28:  $W_{max} = W_n$ 
29:  $Next_n = n$  //selecting next hop node ( $Next_n$ ).
30: End if
31: End while
32: Forward Packet to  $Next_n$ 
33: Return Greedy-Forward-Success
End Algorithm

```

Fig. 1. Pseudocode of Proposed Greedy Forwarding Approach

```

Algorithm: Adaptive-Greedy-Forwarding (Packet)
1:  $R_S$ : Set of neighbor nodes' for S.
   //Phase 2: Find target neighbors of source S.
2: While ( $n \in R_S$ )
3:    $D_n^d = \text{DISTANCE}(P_n, P_d)$  //Equ.14,15
4:    $D_r = \text{RATIO}(D_n^d, D_s^d)$  //Equ.16
5:   If ( $D_r < 1$ )
6:      $N_D \leftarrow n$  //  $N_D$ : Set of nodes closer to destination than source S.
7:   End if
8: End While
9: If ( $N_D == 0$ ) //No nodes closer to destination found
10:  Forward.Mode = Perimeter //Change to Perimeter mode
11:  Return Greedy-Forward-Failure
12:  Break
13: End If
14: While ( $n \in N_D$ )
15:   $Dir(n, d) = \text{DIRECTION}(D_n^d)_{t0, t1} * A(n, d)_{t0, t1}$  //Equ.17,18
16:   $Dir_r = \text{RATIO}(Dir(n, d)_{t0}, Dir(n, d)_{t1})$  //Equ.19
17:  If ( $Dir_r < 1$ )
18:     $T \leftarrow n$  //T: Set of target nodes for source s.
19:  End if
20: End While //Phase 3: Create weight matrix and select next hop.
21: While ( $n \in T \ \& \ N_D$ )
22:   $Weight(n) = \frac{1}{V_{sn}} + G_n + C_n$ 
23:   $W_{matrix} = \{n.Weight(n)\}$  //  $W_{matrix}$  is weight matrix.
24: End While
25:  $W_{max} = 1$  //  $W_{max}$  is the maximum weight value.
26: While ( $n \in W_{matrix}$ )
27:   If  $Weight(n) \geq W_{max}$ 
28:      $W_{max} = W_n$ 
29:      $Next_n = n$  //selecting next hop node ( $Next_n$ ).
30:   End if
31: End while
32: Forward Packet to  $Next_n$ 
33: Return Greedy-Forward-Success
End Algorithm

```

**Table 1.** Beacon packet variables

n Node ID	De-Congestion Level	Node Connectivity	Radio Rang	Position Coordinates	Velocity	Direction Angle	Time
$n$	$G_n$	$C_n$	$r_n$	$P_n(x_n, y_n)$	$v_n$	$a$	$t_s$

The following subsections describe phases of proposed greedy forwarding model implemented within enhanced GPSR:

• **Phase I: Initialization and Update**

Each GPSR node will utilize GPS capability to compute its coordinates, moving direction and speed. Node’s connectivity level, radio range and De-Congestion level is also measured. Afterwards, nodes will encapsulate this information into beacon packets which are periodically broadcasted using flooding method to adjacent nodes according to BUI. Content of beacon message as in proposed model is described in table 1.

After receiving beacon packets, each node will update its routing table after receiving beacon packets from its neighboring nodes. Source node will extract its neighboring nodes' information (defined  $R_s$ ) and start target neighbors' selection phase. Initialization and update phase will continue on-demand based on BUI.

• **Phase II: Finding Target Neighbor**

An important step in proposed greedy forwarding model is to find list of target neighbor nodes for source node  $S$ , denoted as  $T$ . This requires distance and direction estimation between source  $S$ , neighbor  $n$ , and destination  $d$  nodes. For more accurate distance estimation, nodes movement velocity and direction angle is considered in the nodes coordinate measurements and distance estimation process. Distance estimation depends on the knowledge of  $S$ ,  $n$ , and  $d$  nodes' location coordinates. Distance estimation process conducted at  $S$  includes the following steps:

1. Estimate the distance between source node  $S$  and destination  $d$ , denoted as ( $D_s^d$ ).
2. Compute the distance between each neighbor  $n$  and destination node  $d$ , denoted as  $D_n^d$ .
3. Compute the ratio between distance computed in steps 1 and 2.

As mentioned in step (1) and (2) distance values are computed using equations (14) and (15) respectively:

$$D_s^d = \sqrt{(x_{t1.s} - x_d)^2 + (y_{t1.s} - y_d)^2} \tag{14}$$

$$D_n^d = \sqrt{(x_{t1.n} - x_d)^2 + (y_{t1.n} - y_d)^2} \tag{15}$$

Where  $t1$  is the current time of measurement. Afterwards, Distance ratio ( $D_r$ ) is computed between  $D_n^d$  and  $D_s^d$  as in below:

$$D_r = \frac{D_n^d}{D_s^d} \tag{16}$$

Neighbor node with distance ratio below 1, will be selected because it refers to nodes being closer to destination than source. Distance calculations are based on updated position information received at  $\mathbf{t1}$  by beacon messages. For neighboring nodes achieving the first condition, the direction ratio ( $\mathbf{Dir}_r$ ) between the old and new moving directions of each neighbor node  $\mathbf{n}$  with reference to destination  $\mathbf{d}$  is computed as follow [12]:

$$\mathbf{Dir}(\mathbf{n}, \mathbf{d})_{\mathbf{t0}} = (\mathbf{D}_n^d)_{\mathbf{t0}} * \mathbf{A}(\mathbf{n}, \mathbf{d})_{\mathbf{t0}} \tag{17}$$

$$\mathbf{Dir}(\mathbf{n}, \mathbf{d})_{\mathbf{t1}} = (\mathbf{D}_n^d)_{\mathbf{t1}} * \mathbf{A}(\mathbf{n}, \mathbf{d})_{\mathbf{t1}} \tag{18}$$

$$\mathbf{Dir}_r = \frac{\mathbf{Dir}(\mathbf{n}, \mathbf{d})_{\mathbf{t1}}}{\mathbf{Dir}(\mathbf{n}, \mathbf{d})_{\mathbf{t0}}} \tag{19}$$

Where  $\mathbf{Dir}(\mathbf{n}, \mathbf{d})_{\mathbf{t0}}$  and  $\mathbf{Dir}(\mathbf{n}, \mathbf{d})_{\mathbf{t1}}$  are the old and new node movement directions respectively.  $\mathbf{A}(\mathbf{n}, \mathbf{d})_{\mathbf{t0}}$ ,  $\mathbf{A}(\mathbf{n}, \mathbf{d})_{\mathbf{t1}}$  are the angles between node  $\mathbf{n}$  and  $\mathbf{d}$  at time  $\mathbf{t0}$  and time  $\mathbf{t1}$  respectively. Afterwards, if the value of  $\mathbf{Dir}_r$  is less than 1, this indicates that neighbor node  $\mathbf{n}$  is approaching destination, if its greater than 1, this means  $\mathbf{n}$  is moving away from the destination, and if its equals to 1 it means  $\mathbf{n}$  was static. Hence, nodes' with  $\mathbf{Dir}_r$  value less than 1 are favorable, because nodes moving toward destination will become closer to destination and will be more suitable to be next hop candidate. Accordingly, neighboring nodes having distance ratio  $\mathbf{D}_r$  and direction ratio  $\mathbf{Dir}_r$  below 1 will be added to target neighbors' list  $\mathbf{T}$ .

• **Phase III: Weight value computation and next hop selection**

For each node within target neighbors list  $\mathbf{n} \in \mathbf{T}$ , a weight value is computed as follows:

$$\mathbf{W}_n(\mathbf{t1}) = \frac{1}{v_{sn}} + \mathbf{G}_n + \mathbf{C}_n \tag{20}$$

Where  $\mathbf{W}_n(\mathbf{t1})$  is the weight value computed based on beacon messages received from target nodes at time  $\mathbf{t1}$ . Weight value consists of three main factors; the first factor accounts for node's mobility and represents the fraction of relative velocity  $\mathbf{V}_{sn}$  between target and source nodes. As mentioned earlier high difference in relative velocity results in route instability due to link breakage. Hence, less relative velocity is desirable to maintain link connectivity. The second factor  $\mathbf{G}_n$  represents decongestion level of target node. The last factor  $\mathbf{C}_n$  describes target node connectivity level. High connectivity and increased decongestion level are required to maintain route performance. Weight values matrix (WVM) for all target nodes at time  $\mathbf{t1}$  is computed at source and is represented as shown below:

$$\mathbf{W}_{matrix} = \begin{bmatrix} \mathbf{W}_1 & \mathbf{1} \\ \vdots & \vdots \\ \mathbf{W}_n & \mathbf{n} \end{bmatrix} \tag{21}$$

Target node with highest weight value will be selected as optimal next hop node. However, if there were no target neighbors found during proposed greedy forwarding

phases, GPSR will switch into using perimeter mode, in which a packet travels successively using a fully connected planer graph. However, when a node closer to destination is found, greedy forwarding strategy will resume.

## 4 Evaluation Methodology

In order to evaluate the proposed AGPSR, a new simulation software was built using C# based on understanding of perimeter and greedy forwarding functionalities described in [37]. In which, both conventional and proposed GPSR protocols were implemented and executed taking into consideration different MANET environmental settings. Table 2 describes default MANET parameters that are kept constant during simulation.

**Table 2.** Overall MANET Simulation Parameters

Constant Simulation Parameters	Value
Simulation time	1000 seconds
Mobility model	Random way point
MAC layer type	IEEE 802.11, IEEE 15.4
Radio range	250 meters
Traffic type	Constant Bit Rate (CBR)
Number of connections	5
Bandwidth of links	2 Mbps
Packet size	512 Byte
Transmission Rate	5 pkts/s
Seed	5, 20, 44, 50, 64, 71, 80, 89, 91, 110

The evaluation work focused towards measuring a set of performance metrics including average E2E delay, PDR, normalized routing load (NRL) and power consumption.

- **PDR** is the ratio between received packets at destination to the total packets being sent by source. PDR measures routing protocol transmission efficiency. PDR is computed as following [38]:

$$PDR = \left( \frac{\sum_{m=1}^n \text{Packets Arrived at Destination}}{\sum_{m=1}^n \text{Packets Transmitted}} \right) * 100\% \quad (22)$$

- **E2E delay** refers to the total time required for the packet to travel from source node to destination. This can consist of several delay components; transmission, retransmission and propagation delays, time required for route discovery, queueing time. The average E2E delay can be computed as follows [38]:

$$E2E = \sum_{m=1}^n \frac{(\text{Recvied Time} - \text{Sent Time})}{\sum_{m=1}^n n \text{ transmissions}} \quad (23)$$

- **NRL** defines the ratio between generated control packets and each data packet delivered at destination. This metric measures the overall network overhead generated by the routing protocol. NRL is computed as follows [38]:

$$NRL = \left( \frac{\sum_{m=1}^n \text{Control Packets}}{\sum_{m=1}^n \text{DataPackets}} \right) \quad (24)$$

- **Average Energy** consumption describes the amount of energy being consumed during a specific time period. Efficient energy consumption at each node is a major factor required for improving network life time. Average energy consumption is computed as follows [38]:

$$AvgEng = \frac{\sum_{m=1}^n (\text{InitialEnergy} - \text{EndEnergy})}{n} \quad (25)$$

- Where **n** is number of nodes

Three different simulation scenarios were implemented, each scenario focused on measuring the effect of different MANET environmental setting on GPSR performance. In the first simulation scenario, different number of nodes were used, while the remaining simulation parameters were constant. Increasing the number of nodes will increase network density. High density will generate more control messages leading to increased network overhead. However, in the second scenario, different network sizes were used and remaining parameters were kept constant. Increasing network size will escalate the travel area of nodes and reduce nodes' connectivity. The last scenario focuses on varying nodes' speed of travel. Increasing node speed will result in high node mobility and frequent network topology changes. Tables 3, 4 and 5 describe varying and fixed simulation parameters used in scenarios 1, 2 and 3 respectively.

**Table 3.** Simulation parameters for scenario 1: Node density

<b>Map size</b>	900×900 m
<b>Number of nodes</b>	30, 50, 70, 90, 110, 130, 150, 170, 200, 230, 250
<b>Mobility speed</b>	70 m/s

**Table 4.** Simulation parameters for scenario 2: Network size

<b>Map size</b>	200×200, 300×300, 400×400, 500×500, 800×800, 1000×1000, 1500×1500, 1750×1750, 2000×2000 m
<b>Number of nodes</b>	110 nodes
<b>Mobility speed</b>	70 m/s

**Table 5.** Simulation Parameters for scenario 3: Node speed

<b>Map size</b>	900×900 m
<b>Number of nodes</b>	110 nodes
<b>Mobility speed</b>	40, 50, 60, 70, 80, 90, 100 m/s

For more effective performance measurement, all three scenarios were integrated, in which the average parameter value of each scenario was used in the other scenario. The

average of network sizes and mobility speeds were utilized while varying node density in scenario 1. In scenario 2, average of node density and speed values were used while varying network size. In addition, average network size and node density values were used while varying node speed in scenario 3.

## 5 Results and Discussion

Each scenario was run 10 times for every value of varying parameter, each time with a different seed. Results described here were obtained by calculating the average of the simulation results.

### 5.1 Scenario 1 results: The impact of node density

The impact of number of nodes on the routing performance of proposed and conventional GPSR in terms of PDR, E2E delay, routing overhead and power consumption is presented in figure 2, 3, 4 and 5.

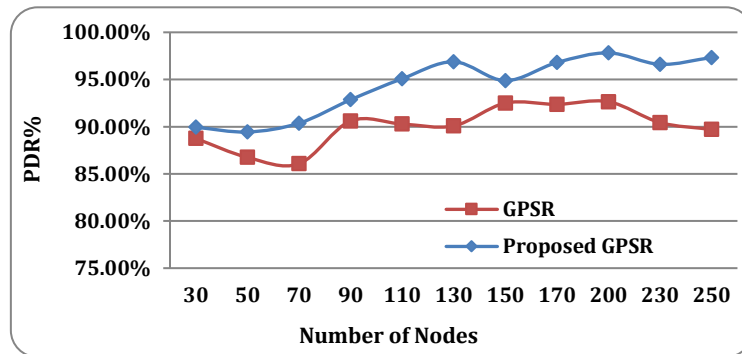


Fig. 2. Impact of node density on PDR for both proposed &conventional GPS

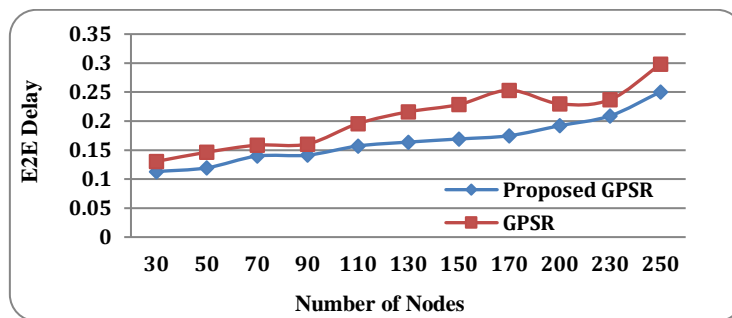


Fig. 3. Impact of node density on E2E delay for both proposed & conventional GPSR

The PDR for both protocols is relatively similar if the number of nodes in the network was below 90. This is due to low overhead which results in more available bandwidth. However, as the quantity of nodes grows, network topology tends to change rapidly especially with increased node mobility, this contributes to the higher overhead and congestion in the network, hence the packet delivery fraction tends to slightly decrease. As shown in figure 2, the proposed GPSR attains higher PDR than conventional GPSR protocols although of increased node density. This is due to the use of the weighted mechanism which has maintained node connectivity, reducing number of link failures and reducing number of hops to destination. Hence, packet loss and packet re-transmissions are significantly decreased. This explains the best E2E performance achieved by proposed GPSR as shown in figure 3. In addition, proposed GPSR utilizes on-demand BUI which efficiently adapts beacon updates with topology changes, resulting in low overhead and allowing more network resources to be available. This justifies the low routing overhead, and reduced overall power consumption achieved by proposed GPSR comparing to conventional GPSR as illustrated in figure 4 and 5 respectively.

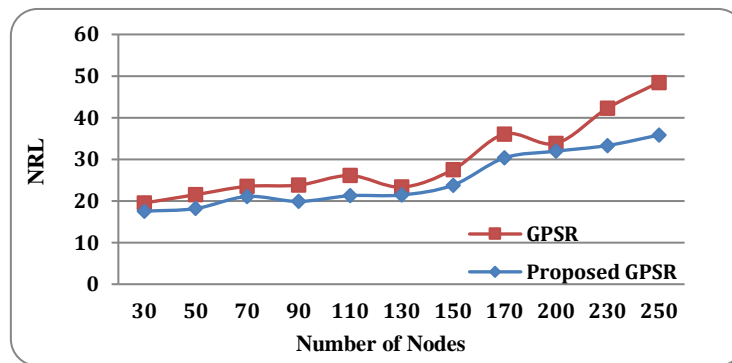


Fig. 4. Impact of node density on NRL for proposed & conventional GPSR

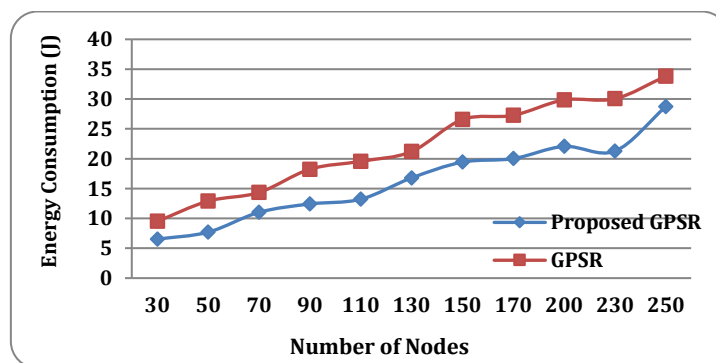


Fig. 5. Impact of node density on Energy Consumption for proposed & conventional GPSR

### 5.2 Scenario 2 results: Impact of network size:

In this scenario, different grid network sizes were used to measure its impact on routing performance. For each network size value, high mobile speed (70) and increased node density (110) values were used.

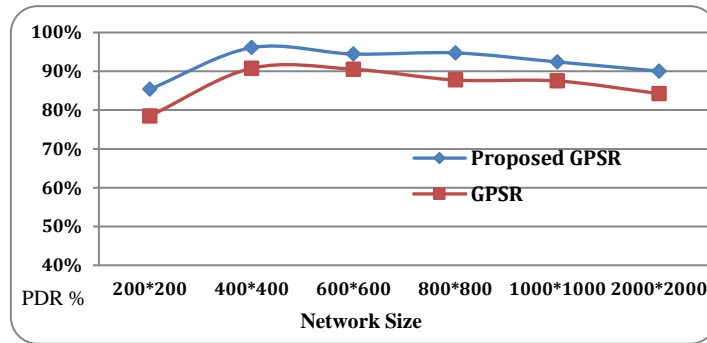


Fig. 6. Impact of Network Size on the PDR for both proposed and conventional GPSR

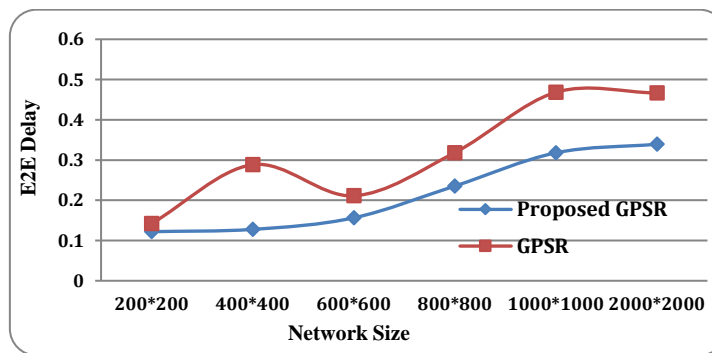


Fig. 7. Impact of Network Size on E2E delay for both proposed and conventional GPSR

Increased network size provides nodes with more freedom to move which leads to continues topology changes, more especially while using high node speeds. Also, during this scenario, links connectivity and reliability was negatively affected, because nodes might have moved out of coverage range of others, and in some cases destination nodes became unreachable, which have resulted in increased packet loss, more packet retransmission and congestion. However, the proposed GPSR was less affected from increased network size. This is due to the use of on demand BUI in initialization phase. Along with utilizing direction ratio and relative velocity in target neighbor selection phase, which allows choosing neighboring nodes moving towards the destination and with same direction as source node.

It is clear from figure 6, proposed GPSR outperformed conventional GPSR in terms of PDR more especially when network size increased over (900x900), in which it shows a steady performance until reaching grid size (2000x2000). As shown in figure 7, E2E

delay tend to slightly drop for both protocols after grid size (1500x1500), however in overall it was clear that proposed GPSR performs best E2E delay achieving average of 0.1 s, comparing to an average of 0.2 s achieved by conventional GPSR. In addition, from figure 8 and figure 9, it can be noticed that for both protocols, NRL and energy consumption grow uniformly along with the network size. However, both performance metrics dramatically increase after grid size 1000x1000.

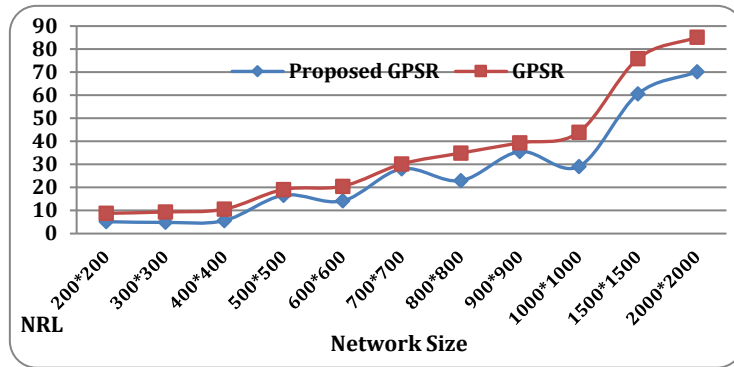


Fig. 8. Impact of Network Size on the NLR for both proposed and conventional GPSR

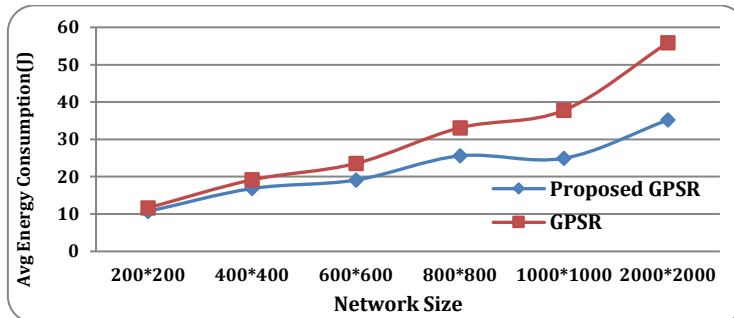


Fig. 9. Impact of Network Size on Energy Consumption for proposed & conventional GPSR

### 5.3 Scenario 3 results: Impact of node mobility

In this scenario, the effect of node mobility is measured under large network size (900x9000m) and highest node density (110 nodes) were fixed and used during all simulation runs. Mobility speed ranges between 40 to 100 m/s. As mentioned before, increased node speed will result in rapid network topology changes and negatively affects links connectivity and reliability. It can be noticed from figure 10, that both protocols achieve a stable PDR performance during the simulation of different network speed, with a slight advantage to the proposed GPSR especially after node speed 70. Also, due to above mentioned advantages of proposed GPSR it outperformed conventional GPSR in terms of E2E delay, routing overhead, and power consumption, as illustrated in figure 11, 12, 13 respectively.

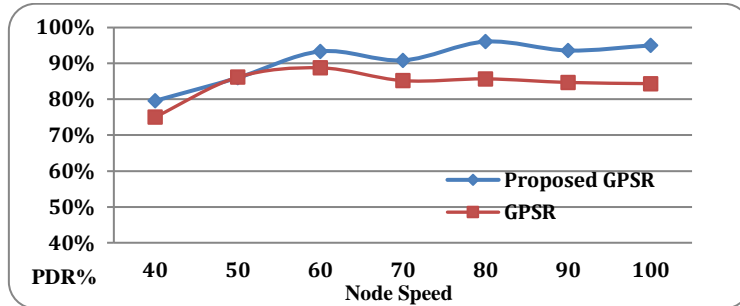


Fig. 10. Impact of Node Speed on PDR for both proposed and conventional GPSR

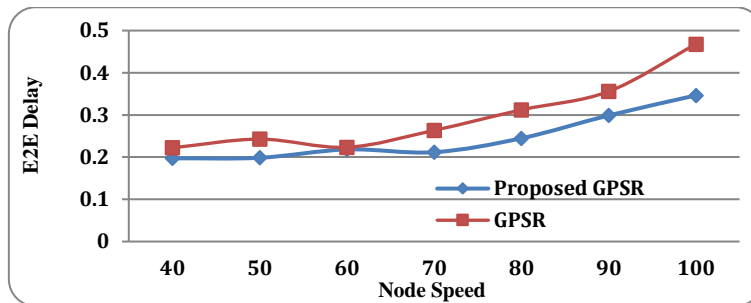


Fig. 11. Impact of Node Speed on E2E delay for both proposed and conventional GPSR

Table 6 below describes the average of overall performance results for scenarios 1, 2 and 3 during all simulation runs and a 95% confidence level. Hop count is a performance metric measuring number of hops to destination. This metric is affected by routing performance and is linked constantly with other matrices including; PDR, E2E delay, power consumption and NRL. Major challenges for both protocols was scenario 3, where high node speeds and large network sizes were implemented. In this scenario, network overhead and power consumption were the highest comparing to other scenarios for both protocols. However, proposed GPSR achieved PDR value of 91%, comparing to conventional GPSR which has achieved 86%.

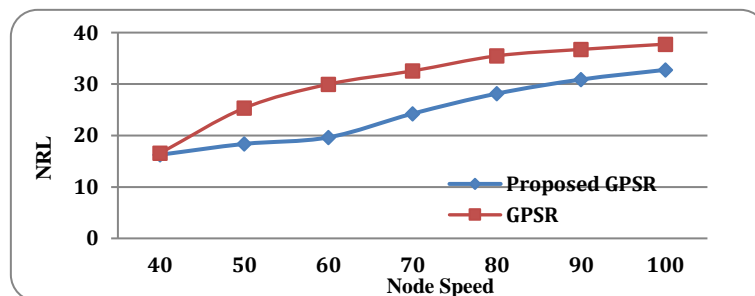


Fig. 12. Impact of Node Speed on the NRL for proposed and conventional GPSR

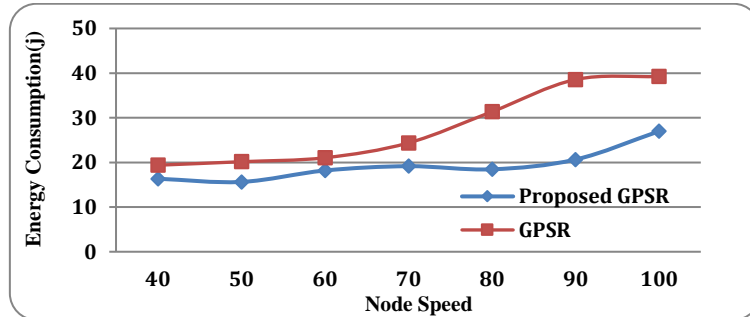


Fig. 13. Impact of Node Speed on Energy Consumption for proposed & conventional GPSR

Table 6. Overall scenarios results

Scenario	PDR		E2E Delay		Power	
	AGPSR	GPSR	AGPSR	GPSR	AGPSR	GPSR
1	94%	90%	0.1	0.2	17	23
2	93%	88%	0.2	0.3	23	30
3	91%	86%	0.3	0.4	25	33
AVG	92.6%	88%	0.2	0.3	21.6	28.6
Scenario	NRL		Hop Count			
	AGPSR	GPSR	AGPSR	GPSR		
1	24	29	3.1	3.4		
2	26	33	3.5	4.6		
3	27	35	4.1	5.1		
AVG	25.6	32.3	3.5	4.4		

It is clear from table 6, the proposed AGPSR has proven its efficiency in improving PDR up-to 4.6 % comparing to conventional GPSR. Certainly, the delay is reduced by AGPSR of up-to 10% compared to conventional GPSR. This delay improvement is linked to the average number of hop count which was reduced by 1.1 % using AGPSR. Routing overhead and power consumption were reduced by nearly 7%. In addition, the performance achieved by AGPSR is considered comparable to other GPSR advancements known as GPSR with k Packets (GPSR-kP) and Path Aware GPSR (PA-GPSR) as described in [39] and [29] respectively. Accordingly, the efficiency and improved performance of AGPSR during different environmental scenarios is confirmed.

## 6 Conclusion

This work presents an improved version of GPSR described as Advanced GPSR (AGPSR). The major improvements of AGPSR were focused towards the greedy forwarding process which was redefined into three operational phases. The first phase is responsible for initializing, updating and broadcasting the beacon packet. More information is added to the beacon packet to account for node density, node mobility and connectivity. The second phase is used to find the target neighbor nodes, these nodes

are having minimum distance to destination and are moving towards the destination. The last phase will utilize up-to-date information available to compute a weight value for each target node. This weight value is used to determine the optimal next hop node.

The computation of this weight value encounters a set of factors including; node density, buffer space, radio range, node mobility including speed and direction. Considering node mobility was important to reduce the possibility of link breakage, and improve location information accuracy. Also, accounting for nodes' available buffer space have lowered congestion level and contributes to the reduced E2E delay experienced. In addition, the concept of relative velocity was used to balance beacon intervals which have decreased network overhead and reduced overall power consumption.

For performance evaluation, a new simulation software was built to implement the AGPSR and conventional GPSR protocols. This simulation tool was used to execute several MANET scenarios including different network sizes, node density and mobility. Results confirm that the proposed AGPSR has achieved an improved performance in terms of PDR, E2E delay, hop count, power consumption, and routing overhead. AGPSR has outperformed conventional GPSR and achieved comparable performance comparing to other GPSR advancement known as GPSR-kP and PA-GPSR.

## 7 References

- [1] Quy, V K. Ban, N T. Nam, V H. Tuan, D M. and Han, N D. (2019). Survey of Recent Routing Metrics and Protocols for Mobile Ad-Hoc Networks. *Journal of Communications*, 14 (2): 110-120. <https://doi.org/10.12720/jcm.14.2.110-120>
- [2] Smiri, S. Boushaba, A. Ben Abbou, R. and Zahi, A. (2018). Geographic and topology-based routing protocols in vehicular ad-hoc networks: Performance evaluation and QoS analysis. *Proceeding of International Conference on Intelligent Systems and Computer Vision (ISCV)*, Fez, April 2-4, pp. 1-8. <https://doi.org/10.1109/isacv.2018.8354070>
- [3] Khalid, H. B., Abdulghani, S. K. M., (2019). Survey of mobile ad hoc networks (MANETS). *International Journal of Engineering and Computer Science*, 8 (2): 24484-24490. <https://doi.org/10.18535/ijecs.v8i02.4229>
- [4] Govindasamy, J., & Punniakody, S. (2017). A comparative study of reactive, proactive and hybrid routing protocol in wireless sensor network under wormhole attack. *Journal of Electrical Systems and Information Technology*, 5 (3): 735-744. <https://doi.org/10.1016/j.jesit.2017.02.002>
- [5] Devi, M. Gill, N. S. (2018). Study of Mobile Ad hoc Network Routing Protocols in Smart Environment. *International Journal of Applied Engineering*, 13(16): 12968-12975.
- [6] Kaplan, E. Hegarty, C. (2005). *Understanding GPS: Principles and Applications*. 2nd edition. Artech House Publishers, London, 3. The State University of New York, Buffalo.
- [7] Cadger, F., Curran, K., Santos, JA., & Moffett, S. (2011). An Analysis of the Effects of Intelligent Location Prediction Algorithms on Greedy Geographic Routing in Mobile Ad-Hoc Networks. In *Unknown Host Publication* (pp. 324-333). University of Ulster, UK: Intelligent Systems Research Centre, Ulster University. <https://doi.org/10.1016/j.adhoc.2015.08.016>
- [8] Wadhwa, D. Deepika, Kochher, V. and Tyagi, R. K. (2014). A Review of Comparison of Geographic Routing Protocols in Mobile Adhoc Network. *Advance in Electronic and Electric Engineering*, 4(1): 51-58.

- [9] Sonam, J. Sandeep S. (2012). Topology vs Position based Routing Protocols in Mobile Ad hoc Networks: A Survey. *International Journal of Engineering Research and Technology (IJERT)*, 1 (3): 1-11.
- [10] Alnabhan, M. Alshuqran, M. Hammad, M. & Al Nawaiseh, M. (2017). Performance Evaluation of Unicast Routing Protocols in MANETs—Current State and Future Prospects. *International Journal of Interactive Mobile Technologies (iJIM)*, 11(1): 84-97. <https://doi.org/10.3991/ijim.v11i1.6295>
- [11] Karp, B. and Kung, H. T. (2000). GPSR: Greedy Perimeter Stateless Routing for Wireless Networks. *Proceedings of the Annual International Conference on Mobile Computing and Networking, Mobicom, 2000*. <https://doi.org/10.1145/345910.345953>
- [12] Kouah, R. Moussaoui, S. Aissani, M. (2012). Direction-based greedy forwarding in mobile wireless sensor networks. *Proceeding of 8th Advanced International Conference on Telecommunications (AICT)*, pp.69-74.
- [13] Purnima, P. K. Umashankar, I. R. IINish, (2014). An Overview of Position Based Routing Protocols in Mobile Ad Hoc Networks. *International Journal of Advanced Research in Computer Science & Technology (IJARCST)*, 2 (2): 148-151.
- [14] AL-Dhief, F. T. Sabri, N. Salim, M.S. Fouad, S. Aljunid, S. A. (2018). MANET Routing Protocols Evaluation: AODV, DSR and DSDV Perspective. *MATEC Web of Conferences, Warsaw, Poland, Volume (150), Article (6024)*. <https://doi.org/10.1051/mateconf/201815006024>
- [15] Patel, H. Kulkarni, G. R. (2017). Enhanced Route Selection Approach of GPSR Routing Protocol in WSN Using Multipath Forwarding in VANET. *International Journal of Advanced Research in Computer Science*, 8(8): 140-145. <https://doi.org/10.26483/ijarcs.v8i8.4772>
- [16] Gupta, A. and Verma, P. (2019). Performance Comparison of Adhoc Networks Routing Protocols., *Proceedings of 2nd International Conference on Advanced Computing and Software Engineering (ICACSE)*, Washington, DC, United States.
- [17] Alabdullah, M. G. Atiyah, B. M. Khalaf, K. S. Yadga, S. H. (2019). Analysis and simulation of three MANET routing protocols: A research on AODV, DSR & DSDV characteristics and their performance evaluation. *Periodicals of Engineering and Natural Sciences*, 7 (4): 1228-1238. <https://doi.org/10.21533/pen.v7i3.717>
- [18] Alnabhan, M. Alsarairh, S. Pattanayak, B. Habboush, A. Hammad, M. (2019). Performance analysis and enhancement of position-based routing protocols in MANETS. *International Journal of Knowledge-based and Intelligent Engineering Systems*, 23 (2): 109-120. <https://doi.org/10.3233/kes-190404>
- [19] Rowaihy, H. BinSahaq, A. (2016). Performance of GPSR and AOMDV in WSNs with Uncontrolled Mobility. *Procedia Computer Science*. 98: 48-55. <https://doi.org/10.1016/j.procs.2016.09.010>
- [20] Setiabudi, A. Pratiwi, A. Ardiansyah, A. Perdana, D. Sari, R. (2016). Performance comparison of GPSR and ZRP routing protocols in VANET environment. *IEEE Region 10 Symposium (TENSYP)*, Bali, Indonesia, June 5 -7. <https://doi.org/10.1109/tenconspring.2016.7519375>
- [21] Kumar, P, Verma, S. (2020). Analysis of OLSR and GPSR Routing Protocols in Airborne Networks for UDP and TCP Environment. *Soft Computing: Theories and Applications*, pp. 205-215. [https://doi.org/10.1007/978-981-15-0751-9\\_19](https://doi.org/10.1007/978-981-15-0751-9_19)
- [22] Alsaqour, R. Zakaria, M. S. Ismail, M. Abdelhaq, M. (2011). Analysis of mobility parameters effect on position information inaccuracy of GPSR position-based MANET routing protocol. *Journal of Theoretical and Applied Information Technology*, 28 (2): 114-120. <https://doi.org/10.1504/ijwmc.2014.058886>
- [23] Bouras, C. Kapoulas, V. Tsanai, E. (2015). A GPSR Enhancement Mechanism for Routing in VANETs. In: Aguayo-Torres M., Gómez G., Poncela J. (eds) *Wired/Wireless Internet*

- Communications. WWIC 2015. Lecture Notes in Computer Science, Vol.9071. Springer, Cham. [https://doi.org/10.1007/978-3-319-22572-2\\_7](https://doi.org/10.1007/978-3-319-22572-2_7)
- [24] Zadina, A. Fevens, T. Bdiri, T. (2016). Impact of Varying Node Velocity and HELLO Interval Duration on Position-based Stable Routing in Mobile Ad Hoc Networks. *Procedia Computer Science*. 94: 353–358. <https://doi.org/10.1016/j.procs.2016.08.053>
- [25] Yang, H. Yu, M. and Zeng, X. (2017). Link available time prediction based GPSR for vehicular ad hoc networks. *Proceeding of IEEE 14th International Conference on Networking, Sensing and Control (ICNSC)*, May 16-18, 2017, Calabria, Southern Italy. pp. 293-298. <https://doi.org/10.1109/icnsc.2017.8000107>
- [26] Zhaoyuan, C. Demin, L. Guanglin, Z. Chang, G. Yong, S. (2016). The Next-Hop Node Selection Based GPSR in Vehicular Ad Hoc Networks. *Journal of Computer and Communications*. 4 (10): pp.44-56. <https://doi.org/10.4236/jcc.2016.410005>
- [27] Wang, C. Fan, Q. Chen, X. Xu, W. (2018). Prediction based Greedy Perimeter Stateless Routing Protocol for Vehicular Self-organizing Network. *IOP International Symposium on Application of Materials Science and Energy Materials (SAMSE)*, pp. 052019. <https://doi.org/10.1088/1757-899x/322/5/052019>
- [28] Silva, A. Niaz, K. M. and Oliveira, A. (2018). An Adaptive GPSR Routing Protocol for VANETs. *Proceeding of 15th International Symposium on Wireless Communication Systems (ISWCS)*. Lisbon, Portugal, August 28-31. <https://doi.org/10.1109/iswcs.2018.8491075>
- [29] Silva, A. & Reza, N. & Oliveira, A. (2019). Improvement and Performance Evaluation of GPSR-Based Routing Techniques for Vehicular Ad Hoc Networks. *IEEE Access*. 7: 21722 – 21733. <https://doi.org/10.1109/access.2019.2898776>
- [30] Bengag, A. Bengag, A. Elboukhari, M. (2020). A novel Greedy Forwarding Mechanism Based on Density, Speed and Direction Parameters for VANETs. *International Journal of Interactive Mobile Technologies*, 14 (8) 2020: pp.196-204. <https://doi.org/10.3991/ijim.v14i08.12695>
- [31] Zhao, L. & Yin, B. & Gao, M. & Zhao, X. (2020). Improved GPSR routing protocol based on weight function in shipborne ad hoc networks. *IOP Conference Series: Materials Science and Engineering*. 768. (2020). <https://doi.org/10.1088/1757-899x/768/5/052134>
- [32] Sekhar, R. Jayudu, N. (2012). D-LAROD: A Density Based LAROD for Geographical Routing in Intermittently Connected MANETs. *International Journal of electronics & communication Technology*, 3 (1): 47-52.
- [33] Tran, D. A. and Raghavandra, H. (2005). Routing with Congestion Awareness and Adaptively in Mobile Ad Hoc Networks. In *Proceedings of wireless communication and networks conferences*. IEEE WCNC. 4: 1988 – 1994.
- [34] Haboush, A. and AlShugran, M. (2018). An Enhanced Queue Management Approach for Greedy Routing in MANETs. *Computer and Information Science*, 11 (2): 64-75. <https://doi.org/10.5539/cis.v11n2p64>
- [35] Alsaqour, R. A. Abdelhaq, M. S. and Alsukour, O. A. (2012). Effect of network parameters on neighbor wireless link breaks in GPSR protocol and enhancement using mobility prediction model. *EURASIP Journal on Wireless Communications and Networking*, Article number:171. <https://doi.org/10.1186/1687-1499-2012-171>
- [36] Al-Mayouf, YRB. Ismail, M. Abdullah, NF. Wahab, AWA. Mahdi, OA. Khan, S. (2016). Efficient and Stable Routing Algorithm Based on User Mobility and Node Density in Urban Vehicular Network. *PLoS ONE*, 11(11): 1-24. <https://doi.org/10.1371/journal.pone.0165966>
- [37] Alvarez-Rohena, M. Eberz, C. (2010). Implementation and Analysis of GPSR: Greedy Perimeter Stateless Routing for Wireless Networks, *IEEE 2010*. <https://doi.org/10.21236/ada440078>

- [38] Bhatia, T. and Verma, A.K. (2015). QoS Comparison of MANET Routing Protocols. International Journal of Computer Network and Information Security, 9: pp.64-73. <https://doi.org/10.5815/ijcnis.2015.09.08>
- [39] Zaimi, I. Houssaini, Z. Boushaba, A. Oumsis, M. (2016). A new Improved GPSR (GPSR-kP) Routing Protocol for Multimedia Communication over Vehicular Ad hoc Network. BDAW '16: Proceedings of the International Conference on Big Data and Advanced Wireless Technologies, Article No: 14. PP. 1–7. <https://doi.org/10.1145/3010089.3010099>

## 8 Author

**Mohammad Alnabhan** is currently an Associate professor of Computer Science at Mutah University, Jordan since 2015. He was appointed as an Assistant Professor at Jerash University, Jordan from 2009 till 2014. In 2009, Alnabhan earned his PhD degree in Computer Science (CS) from Brunel University, UK. His research interest includes mobile computing, context adaptive computing, QoS in wireless networks, and network security.

Article submitted 2020-06-27. Resubmitted 2020-08-03. Final acceptance 2020-08-06. Final version published as submitted by the authors.